Observation of multiple quantum transitions in magnetic nanoparticles

N. Noginova,[1] T. Weaver,[1] E. P. Giannelis,[2] A. B. Bourlinos,[3] V. A. Atsarkin,[4] and V. V. Demidov[4]
[1]*Norfolk State University, Norfolk, Virginia 23504, USA*
[2]*Cornell University, Ithaca, New York 14853, USA*
[3]*Institute of Materials Science, NCSR Demokritos, Athens 60228, Greece*
[4]*Institute of Radio Engineering and Electronics RAS, Moscow 125009, Russia*
(Received 31 August 2007; revised manuscript received 12 November 2007; published 3 January 2008)

Absorption at multiple resonance frequencies is observed in magnetic nanoparticles in strong similarity with forbidden multiple quantum transitions known for paramagnetic ions. Temperature and concentration dependences have been studied to reveal the origin of the signals. The results are discussed using a "quantization" approach, considering resonance transitions between energy levels of a giant spin corresponding to the total magnetic moment of a nanoparticle. The multiple quantum transitions are ascribed to both the effects of anisotropy and dipole-dipole interactions between nanoparticles.

DOI: 10.1103/PhysRevB.77.014403 PACS number(s): 75.20.−g, 75.50.Tt

Transition from quantum dynamics of one or several interacting quantum objects to classical thermodynamics of multiparticle systems is among the most interesting and general problems of fundamental physics. With the development of nanotechnology, more and more experimental studies are conducted in this boundary area, including experiments with magnetic nanoscale objects. Such systems vary from the clusters coupled by strong exchange interactions in crystals with paramagnetic impurities to molecular magnets and further to superparamagnetic nanoparticles containing hundreds or thousands of exchange-coupled spins.

Electron magnetic resonance (EMR) is a convenient method to study magnetic behavior and spin dynamics in nanoscale magnetic systems. The opportunity to use both quantum and classical descriptions makes EMR an excellent tool to study spin systems in the range of quantum-to-classical transition, where classical and quantum considerations can both be applied and compared with each other. Recent years, typical quantum effects such as tunneling and quantum interference were found in molecular magnets containing 10–12 coupled spins (see, for example, Refs. 1). In larger objects, such as nanoscale ferro- (ferri)magnetic particles, analysis of possible quantum effects is more complicated and is not yet fully supported with experimental data. Theoretical approaches based on computer simulations[2–4] concentrate on the analysis of static magnetization and relaxation, while the magnetic resonance is mainly considered from purely classical point of view.[5–9] Note that numerous experimental EMR spectra in magnetic nanoparticles (see, for example, Refs. 10–18) do not well correspond to the theoretical predictions.

An alternative approach is also used,[19,20] where a nanoparticle is being considered as a giant exchange-coupled cluster consisting of N atomic spins s. Only the lowest multiplet is populated, with $S \sim Ns$. In the case of axial symmetry with an easy axis $\boldsymbol{n}$, the behavior of such a system is described with the standard "paramagnetic" spin Hamiltonian as

$$\hat{H}/\hbar = \gamma(\vec{B} \cdot \vec{S}) + D[\hat{S}_n^2 - S(S+1)/3)], \qquad (1)$$

where γ is the electron gyromagnetic ratio, $\hbar$ is the Plank constant, $\boldsymbol{B}$ is the external magnetic field, and D is the effective anisotropy constant. This is a simplified approach; it does not take into account the upper multiplets with different S and neglects contributions from spin waves. However, it describes well the temperature and field dependences of the nanoparticle magnetization.[19] Spin Hamiltonian [Eq. (1)] was successfully used as well, to analyze the field and temperature dependences of the nuclear spin relaxation rates in suspensions of magnetic nanoparticles (magnetic resonance imaging contrast agents).[20]

Such "quantization" consideration differs in some respects from the classical description. The classical picture considers the magnetic energy of a ferromagnetic particle as a continuous energy band. The Landau-Lifshitz equation is used to describe the dynamics; damping is introduced phenomenologically with longitudinal and transverse relaxation rates of the same order and defined through each other. In contrast, the quantization approach describes the situation when there are distinct energy levels characterized by magnetic quantum numbers m, the lifetime on each level being long enough to consider the population at each energy level separately. Spin relaxation is described by the Bloch equations, with the longitudinal (energy) relaxation time T_1 being, in some cases, much longer than the transverse (phase) relaxation time T_2.

In our previous work,[21] we applied and compared both approaches for the description of the EMR signal observed in superparamagnetic nanoparticles[22] and demonstrated that the quantization approach [Eq. (1)] can describe adequately major features of the EMR line shape and its temperature behavior. Besides, the T_1 value was measured and found to be considerably longer than T_2. In the present study, we report results of the EMR experiments with the superparamagnetic nanoparticles and discuss features related to quantal behavior of these systems, similar to those observed in clusters coupled by strong exchange interactions and molecular magnets.

The superparamagnetic nanoparticles used in the experiments were the maghemite (γ-Fe_2O_3, T_C=860 K) nanoparticles with the surface treated with an organic corona. Two series of samples from two different preparation runs (series 1 and series 2) with nominally the same composition and particle size were used. Synthesis and characterization of the

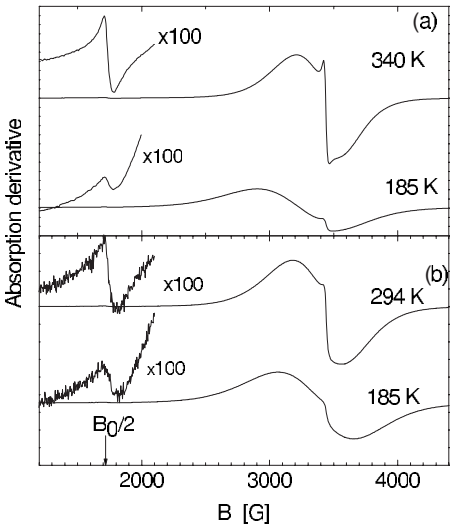

FIG. 1. EMR spectra of the maghemite nanoparticles (series 1) in (a) toluene and (b) polymer. Temperatures are indicated in the figure.

particles are described in Ref. 21. According to transition electron microscopy characterization, the particles are nearly spherical, with the mean diameter of 4.8 nm and log-normal dispersion $\sigma=0.15$. Dense ferrofluid has nanoparticle content around 40 wt %. To prepare experimental samples with different concentrations, the ferrofluid was dispersed in liquid (toluene) and solid (polystyrene) matrices. The electron magnetic resonance studies were performed using a Bruker EMX spectrometer operating at $\omega/2\pi=9.8$ GHz (X band). A commercial gas-flow cryostat and ARS closed-circle cryostat CSW-202AE were used in the variable temperature experiments.

Typical EMR signals are shown in Fig. 1. As one can see, the major spectral feature is observed around g factor of 2. It consists of a broad slightly asymmetric component and a narrow feature. With decrease in temperature, the broad component becomes much broader and symmetric, while the narrow component quickly decreases in amplitude, keeping practically the same width. These general features are consistent with the experimental data reported by other authors.[11,13,14,16,17]

The temperature dependence of the total intensity I (determined through double integration of the curve) is described with the Langevin function, $L(\mu B_0/k_BT)$, with $\mu B_0/k_B=760\pm100$ K (here, μ is the magnetic moment of the particle, B_0 is the resonance field, and k_B is the Boltzmann constant). The intensity of the narrow feature in both liquid and solid systems can be described with the activation law as $\exp(-E_a/k_BT)$ with the characteristic temperature, $E_a/k_B \sim 850$ K (series 1) and ~ 780 K (series 2). Note that these values are very close to the temperature coefficient $\mu B_0/k_B$, obtained from the fitting of the total intensity.

The detailed description and discussion of these major features at $g=2$ is published in Ref. 21. The quantization approach was used based on summation of the resonance transitions over the whole energy spectrum given by the spin Hamiltonian [Eq. (1)], with proper account for the equilibrium populations and transition probabilities. This allowed to explain the double-feature shape of the main EMR signal and its temperature behavior. In particular, the narrow component results from the contribution of the states with small $|m_i|$, which are not much affected by the anisotropy field and thus not broadened by the random distribution of the symmetry axes. Since these states lie well above of the ground energy level, the intensity of the narrow feature decreases exponentially upon cooling.

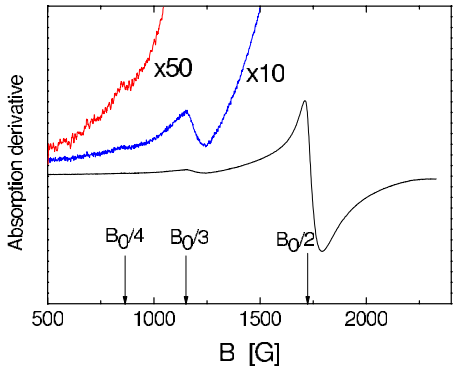

FIG. 2. (Color online) Multiple quantum transitions ($k=2,3,4$) in the suspension of the nanoparticles in toluene (series 2).

Let us now concentrate on the main subject of this paper, the spectral lines observed at the lower fields, $B_{0k}=B_0/k$, where B_0 is the resonance field of the main resonance and k are integer numbers, 2, 3, and 4 (see Fig. 2). The operating frequency of the EMR spectrometer is kept constant, thus these lines correspond to the transitions at the double, triple, etc., resonance frequencies. Their intensities decrease sharply with k increasing, the relative magnitudes being independent on the microwave power. The latter enables one to exclude the spin-wave resonances and other nonlinear ferromagnetic resonance effects. Such multiple quantum transitions are well known in electron paramagnetic resonance (EPR) spectroscopy,[23] where they are explained with the nonsecular terms in the crystal field and dipolar interaction between paramagnetic centers.

In similarity with EPR, let us refer to those signals as multiple quantum transitions, 2Q, 3Q, 4Q, and the main signal as 1Q. As far as we know, no study of such effects in relatively large magnetic objects such as magnetic nanoparticles has been reported to date. According to our recent results, similar features with $g\approx3.97$ can be observed in nanoparticles of different types and sizes, in particular, magnetite nanoparticles with rather broad distribution of the particle size around the mean value of $d=9$ nm.[24] The intensity of the 2Q peak as well as the intensity of the narrow spectral component at $g=2$ are considerably lower in magnetite systems than in maghemite particles of smaller size. Besides, the Fe_3O_4 systems demonstrate additional low-field signals as well, with $g=4.3$ of clearly paramagnetic nature, which can be ascribed to the residue of the isolated Fe^{3+} ions.[16,24]

Figure 3 demonstrates the temperature dependence of the double integrated intensity of 2Q resonance line normalized to the intensity of the major component 1Q, both in the dense and diluted samples. The ratio I_{2Q}/I_{1Q} is nearly constant at higher temperatures and steeply decreases in the low-

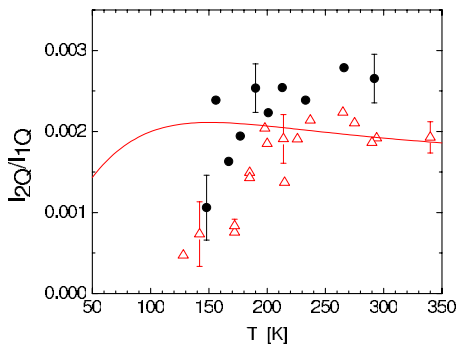

FIG. 3. (Color online) Temperature dependence of the relative intensity of 2Q resonance in dense ferrofluid (circles) and diluted in polymer with $c=0.01$ wt % (triangles), series 1. The curves are calculated using Eq. (3) (solid line) and Eq. (4) (dotted line).

temperature range. Note, however, that the experimental error grows considerably at low temperatures due to broadening and overlapping of the 1Q and 2Q signals.

The dependence of I_{2Q}/I_{1Q} on the concentration c of the nanoparticles is shown in Fig. 4. As one can see, the relative intensity of the signal slightly grows with increase in c, pointing to the role of the interparticle interactions. The shape of the 2Q line depends on the concentration as well: the narrow component becomes more pronounced in well-diluted samples.

Let us discuss the obtained results and try to interpret them based on the spin Hamiltonian [Eq. (1)], corresponding to the lowest multiplet of a large exchange-coupled cluster. In the reference frame with the axis z directed along $\boldsymbol{B}$ and making angle θ with the anisotropy axis $\boldsymbol{n}$, one gets,[25]

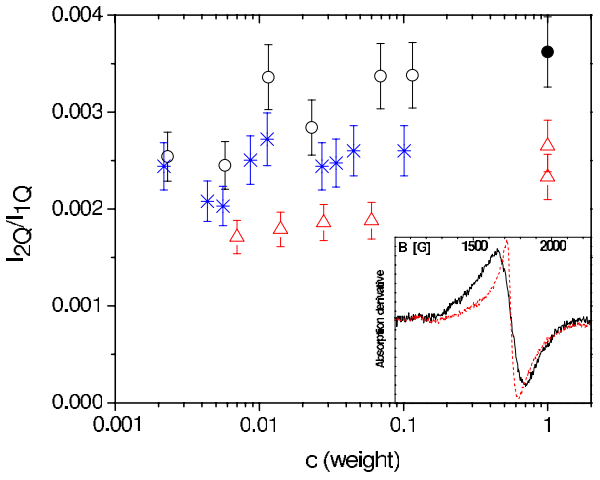

FIG. 4. (Color online) Concentration dependence of the relative intensity I_{2Q}/I_{1Q} at room temperature. Triangles: diluted in toluene and dense liquid; stars: diluted in polymer, series 2. Open circles: diluted in polymer; filled circle: dense liquid, series 1. Inset: 2Q signal in dense ferrofluid (solid trace) and diluted in polymer with $c=0.01$ (dotted).

$$\hat{H}/\hbar = \gamma B\hat{S}_z + \frac{D}{2}\left\{(3\cos^2\theta - 1)\left[\hat{S}_z^2 - \frac{S(S+1)}{3}\right] + \sin\theta\cos\theta[\hat{S}_z(\hat{S}_+ + \hat{S}_-) + (\hat{S}_+ + \hat{S}_-)\hat{S}_z] + \frac{\sin^2\theta}{2}(\hat{S}_+^2 + \hat{S}_-^2)\right\}. \quad (2)$$

The bulk anisotropy of maghemite is weak and cubic,[26] but surface effects in small particles are known to cause some additional axial anisotropy.[4,11,27] Here, for simplicity, we consider axial anisotropy with $S|D| \ll \gamma B$. In the zeroth approximation, the energy levels are determined by the first two terms of Eq. (2) and correspond to the eigenvalues m of the operator S_z. The microwave field, $\boldsymbol{B}_1 \exp(i\omega t)$ perpendicular to z, induces the allowed transitions with $\Delta m = \pm 1$. Transitions with $\Delta m = \pm 2$ are forbidden in this approximation but would be allowed within the first-order perturbation theory, considering admixing of the adjacent states $|m \pm 1\rangle$ due to the nondiagonal matrix elements of the operators $\hat{S}_z\hat{S}_\pm$ [the third term in Eq. (2)]. The probabilities of the transitions, $m \to m+2$, induced by the microwave field $\boldsymbol{B}_1 \exp(2i\gamma Bt)$ can be calculated in the first order of perturbation theory.[23] To find the total intensity of the 2Q transitions, one should perform summation of the transition probabilities over m, taking into account the thermal distribution of the energy level populations. Assuming $S \gg 1$, we get

$$\left(\frac{I_{2Q}}{I_{1Q}}\right)_{aniso} = 8\sin^2\theta\cos^2\theta\left(\frac{B_a}{B_0}\right)^2\frac{[\xi - 3L(\xi)]}{\xi^2 L(\xi_0)}, \quad (3)$$

where $\xi = MVB_0/2k_BT$, $\xi_0 = 2\xi$, and $B_a = -2SD$ (this term corresponds to the anisotropy field in classical description). At random orientations of the anisotropy axes, the numeric factor in Eq. (3) is averaged to 16/15.

Another reason why the forbidden multiple quantum transitions may become allowed is the magnetic dipole-dipole interactions between particles. The corresponding spin Hamiltonian[23] contains two-particle operators $\hat{S}_{i\alpha}\hat{S}_{j\beta}$, where $\alpha, \beta = z, +, -$, and indices i, j correspond to interacting particles at the distance r_{ij}. In this case, the 2Q resonance absorption becomes possible due to the terms $\hat{S}_{zi}\hat{S}_{\pm j} + \hat{S}_{\pm i}\hat{S}_{zj}$ corresponding to $\Delta m_i = \Delta m_j = \pm 1$. As a result, we get

$$\left(\frac{I_{2Q}}{I_{1Q}}\right)_{dip} = 2\left(\frac{3MV\sin\theta_{ij}\cos\theta_{ij}}{Br_{ij}^3}\right)^2\frac{[L(\xi)]^2}{\xi L(\xi_0)}, \quad (4)$$

where θ_{ij} is the angle between $\mathbf{r}_{ij}$ and $\mathbf{B}$. The summation over i, j should be performed when a number of particles are interacting. Multiple quantum transitions with $k=3,4$ (Fig. 2) can be obtained from the same Hamiltonian with the perturbation theory of higher orders.

Equations (3) and (4) have similar temperature dependences. Both predict saturation to a constant at high temperatures ("paramagnetic limit," $\xi \ll 1$), a dull maximum at $\xi \sim 0.2$, and decrease to zero as $\sim T$ at low temperatures ("ferromagnetic" limit, $\xi \gg 1$). Typical curves calculated with Eqs. (3) and (4) are shown in Fig. 3. In both cases, the value of $MVB_0/k_B = 800$ K was used. The solid curve corresponds to Eq. (3) with $B_a = 450$ G. The dotted curve was calculated

using Eq. (4). In this case, the angular dependence was averaged to 2/15, and only four nearest neighbors were taken into account with $r_{ij}^{\min}=8.4$ nm.

A qualitative agreement with the experiment can be seen at high temperatures; however, in the low-temperature range, the decrease of the 2Q signal is much steeper than predicted, thus resembling the temperature behavior of the narrow spectral feature at $g=2$. Unfortunately, the broadening and overlapping of the main and 2Q resonances do not allow us to obtain accurate estimations in the low-temperature range.

Besides, the multiple quantum signals are not shifted to lower fields upon cooling, similarly to the narrow 1Q feature and in contrast with the broader EMR component. This correlation between the narrow 1Q component and 2Q signal can be explained by the role of the central (low-$|m|$) states of the ground spin multiplet. According to our model, these states are responsible for the narrow 1Q peak and, at the same time, provide the maximum multiple-quantum probabilities. It should also be noted that numerical modeling performed for $S\leqslant 100$ in Ref. 28 predicts pronounced quantal effects for small $|m|$'s and transfer to classical behavior as $|m|$ increases. Significantly, lower intensities of the narrow component and 2Q signal observed in the particles of larger size[25] are consistent with this model and indicate weakening of the quantum features with increase in particle size.

The concentration dependence of the 2Q signal (Fig. 4) indicates that both the anisotropy and dipole-dipole mechanism make comparable contributions, with the dipole-dipole mechanism playing more pronounced role in high-density samples. Estimation of the anisotropy field using Eq. (3) yield $B_a\cong 500$ G, which is in agreement with the earlier estimations[21] based on the spectral shape of the EMR spectra in the same material. Assuming that nearest neighbors contribute the most to the dipole mechanism, the average distance between the two nearest particles can be estimated from Eq. (4) as $r_{ij}^{\min}\sim 8$ nm. This seems reasonable for our materials, where nanoparticles are covered with an organic corona preventing tight contact. Also, this is in good agreement with the estimation of $r_{ij}^{\min}$ from the analysis of the EMR and optical experiments with the field-induced orientation of the aggregates (chains) consisting of a number of dipolar-coupled nanoparticles.[21,29] According to the angular dependence of 2Q probability [Eq. (4)], partial alignment of the dipolar-coupled chains along $\boldsymbol{B}$ can decrease the 2Q intensity in liquid suspensions as compared to solid ones; this agrees with the experimental data shown in Fig. 4.

Note that, according to Eq. (3), the 2Q probability falls to zero both at $\theta=0$ and $\pi/2$. As a result, the inhomogeneous broadening caused by random orientation of the anisotropy axis is greatly reduced. Further, the homogeneous part of the 2Q linewidth in the magnetic-field units should be half the 1Q one because of $g=4$ instead of 2. As a result, the 2Q line is expected to be relatively narrow, in good agreement with the experiment.

In conclusion, multiple quantum resonances with $k=2$, 3, and 4 have been found in the EMR spectra of maghemite nanoparticles dispersed in solid and liquid media. At higher temperatures, both the intensity and the line shape of the 2Q line are consistent with the model based on the spin Hamiltonian related to the ground spin multiplet of a particle considered as a giant cluster coupled by exchange interactions. The fitting parameters, such as the anisotropy and dipolar fields, correspond well to independent estimations. The quantitative agreement is broken, however, at low temperatures, where the intensity of the low-field features sharply decreases. Further studies, both experimental and theoretical, would provide more insight to the behavior of such boundary multispin systems.

The authors are grateful to F. S. Dzheparov for helpful discussions. The work was partly supported by National Science Foundation (NSF) CREST Project HRD-9805059, NSF PREM under Grant No. DMR-0611430, Russian Foundation for Basic Research (Grant No. 05-02-16371), and Russian Academy of Sciences (Programs P03-02-2.24 and Spintronics No. 1-18).

[1] *Quantum Tunneling of Magnetization*, edited by L. Gunther and B. Barbara (Kluwer, Dordrecht, 1995); E. M. Chudnovsky, Science **274**, 938 (1996); P. C. E. Stamp, Nature (London) **383**, 125 (1996); L. Thomas, F. Lionti, R. Ballou, D. Gatteschi, R. Sessoli, and B. Barbara, *ibid.* **383**, 145 (1996); D. Gatteschi, J. Alloys Compd. **317-318**, 8 (2001); S. J. Blundell and F. L. Pratt, J. Phys.: Condens. Matter **16**, R771 (2004); W. Wernsdorfer, M. Murugesu, and G. Christou, Phys. Rev. Lett. **96**, 057208 (2006); R. López-Ruiz, F. Luis, A. Millán, C. Rillo, D. Zueco, and J. L. García-Palacios, Phys. Rev. B **75**, 012402 (2007).

[2] D. A. Dimitrov and G. M. Wysin, Phys. Rev. B **51**, 11947 (1995).

[3] R. H. Kodama and A. E. Berkowitz, Phys. Rev. B **59**, 6321 (1999).

[4] D. A. Garanin and H. Kachkachi, Phys. Rev. Lett. **90**, 065504 (2003).

[5] Yu. L. Raikher and V. I. Stepanov, Sov. Phys. JETP **75**, 764 (1992).

[6] Yu. L. Raikher and V. I. Stepanov, Phys. Rev. B **50**, 6250 (1994); J. Magn. Magn. Mater. **149**, 34 (1995).

[7] J. L. Dormann, F. D'Orazio, F. Lucari, E. Tronc, P. Prené, J. P. Jolivet, D. Fiorani, R. Cherkaoui, and M. Noguès, Phys. Rev. B **53**, 14291 (1996).

[8] E. de Biasi, C. A. Ramos, and R. D. Zysler, J. Magn. Magn. Mater. **262**, 235 (2003).

[9] K. D. Usadel, Phys. Rev. B **73**, 212405 (2006).

[10] E. P. Valstyn, J. P. Hanton, and A. H. Morrish, Phys. Rev. **128**, 2078 (1962).

[11] F. Gazeau, J. C. Bacri, F. Gendron, R. Perzynski, Yu. L. Raikher, V. I. Stepanov, and E. Dubois, J. Magn. Magn. Mater. **186**, 175 (1998).

[12] B. Martinez, X. Obradors, L. Balcells, A. Rouanet, and C. Monty, Phys. Rev. Lett. **80**, 181 (1998).

[13] F. Gazeau, V. Shilov, J. C. Bacri, E. Dubois, F. Gendron, R. Perzynski, Yu. L. Raikher, and V. I. Stepanov, J. Magn. Magn.

Mater. **202**, 535 (1999).
[14] D. Prodan, V. V. Grecu, M. N. Grecu, E. Tronc, and J. P. Jolivet, Meas. Sci. Technol. **10**, L41 (1999).
[15] Yu. A. Koksharov, S. P. Gubin, I. D. Kosobudsky, G. Yu. Yurkov, D. A. Pankratov, L. A. Ponomarenko, M. G. Mikheev, M. Beltran, Y. Khodorkovsky, and A. M. Tishin, Phys. Rev. B **63**, 012407 (2000).
[16] R. Berger, J.-C. Bissey, J. Kliava, H. Daubric, and C. Estournés, J. Magn. Magn. Mater. **234**, 535 (2001); R. Berger, J. Kliava, and J.-C. Bissey, J. Appl. Phys. **87**, 7389 (2000).
[17] R. V. Upadhyay, Kinnari Parekh, and R. V. Mehta, Phys. Rev. B **68**, 224434 (2003).
[18] P. Dutta, A. Manivannan, M. S. Seehra, N. Shah, and G. P. Huffman, Phys. Rev. B **70**, 174428 (2004).
[19] D. A. Dimitrov and G. M. Wysin, Phys. Rev. B **54**, 9237 (1996).
[20] A. Roch and R. N. Muller, J. Chem. Phys. **110**, 5403 (1999).
[21] N. Noginova, F. Chen, T. Weaver, E. P. Giannelis, A. B. Bourlinos, and V. A. Atsarkin, J. Phys.: Condens. Matter **19**, 246208 (2007).
[22] A. B. Bourlinos, R. Herrera, N. Chalkias, D. D. Jiang, Q. Zhang, L. A. Archer, and E. P. Giannelis, Adv. Mater. (Weinheim, Ger.) **17**, 234 (2005).
[23] A. Abragam and B. Bleaney, *Electron Paramagnetic Resonance of Transition Ion* (Clarendon, Oxford, 1970), Chap. 9.
[24] Maxim M. Noginov, N. Noginova, O. Amponsah, R. Bah, R. Rakhimov, and V. A. Atsarkin, arXiv:0711.0168 (unpublished).
[25] A. Abragam, *The Principles of Nuclear Magnetism* (Clarendon, Oxford, 1963), Chap. VI.
[26] J. B. Birks, Proc. Phys. Soc. London, Sect. B **63**, 65 (1950).
[27] L. Néel, J. Phys. Radium **15**, 224 (1954).
[28] J. L. Garcia-Palacios and S. Dattagupta, Phys. Rev. Lett. **95**, 190401 (2005).
[29] N. Noginova and J. McClure, Physica B **393**, 43 (2007).